ELSEVIER

Journal of Physics and Chemistry of Solids 61 (2000) 899–906

JOURNAL OF PHYSICS AND CHEMISTRY OF SOLIDS

www.elsevier.nl/locate/jpcs

Structural studies of $KNbO_3$ in niobate glass-ceramics

J.S. de Andrade[a,b], A.G. Pinheiro[a], I.F. Vasconcelos[a], M.A.B. de Araújo[a], M.A. Valente[c], A.S.B. Sombra[a,*]

[a]*Laboratório de Óptica não Linear e Ciência dos Materiais (LONLCM), Departamento de Fisica, Universidade Federal do Ceará, Caixa Postal 6030, CEP 60455-760 Fortaleza, Ceará, Brazil*

[b]*Centro de Tecnologia, Universidade de Fortaleza (UNIFOR), Fortaleza, Brazil*

[c]*Departamento de Física, Universidade de Aveiro, Campus Universitário de Santiago, 3810 Aveiro, Portugal*

Received 5 August 1999; received in revised form 12 October 1999; accepted 12 October 1999

Abstract

Potassium niobophosphate glasses and glass-ceramics of the family $[xNb_2O_5\cdot(50-x)P_2O_5\cdot 50K_2O]{:}yFe_2O_3$ were studied by X-ray powder diffraction, Mössbauer, infrared and Raman scattering spectroscopy. For the potassium–phosphate samples $[50P_2O_5–50K_2O]$, the iron oxide presents a network forming behavior for 5 mol% of Fe_2O_3 doping. From our Mössbauer analysis, high spin Fe^{2+} and Fe^{3+} in a distorted octahedral coordination are present in all samples. One can conclude from the Mössbauer parameters that iron is present in a very broad site distribution, which is characteristic of an amorphous structural neighborhood. The precipitation of crystalline $K_4Nb_6O_{17}$ and the ferroelectric $KNbO_3$ crystals was confirmed by X-ray powder diffraction in the samples with $x = 40$ and 50 mol%, respectively. The infrared and Raman scattering spectroscopy results suggest that the increase of the ratio Nb_2O_5/P_2O_5 leads the niobium to sites of octahedral symmetry and consequently to the formation of ferroelectric $KNbO_3$, as seen by X-ray diffraction analysis.

Keywords: Ferroelectric $KNbO_3$; A. Glasses; A. Ceramics

1. Introduction

In recent years, glasses containing Nb_2O_5 are of great interest, because of their application as nonlinear photonic materials [1–5], and as laser hosts having high nonlinear optical parameters [6]. However, unlike silicate and phosphate-based glasses, very little research has been done on niobate-based glasses. The role played by Nb_2O_5 in the glass structure, the coordination-state of Nb^{5+}, and the interaction with other elements in the glass network, is still a subject under study. Studies on the niobate glasses [7] $P_20_5–Nb_2O_5–V_20_5–TiO_2$ and $P_20_5–Nb_2O_5–TiO_2–Fe_2O_3$, by infrared (IR) spectroscopy, have found evidence of the existence of NbO_4 and NbO_6 units. The existence of NbO_6 polyhedral in the glass network of $K_2O–Nb_2O_5–SiO_2$ was confirmed using Raman spectroscopy [8]. The effect of iron doping and associated vacancies in $P_2O_5–PbO–Nb_2O_5–K_2O–Fe_2O_3$ glasses has been studied by thermally stimulated depolarization currents and Mössbauer spectroscopy [9]. In Ref. [10] we did a study of lithium niobium–phosphate glasses $Nb_2O_5–P_2O_5–Li_2O{:}Fe_2O_3$ using ^{57}Fe Mössbauer and IR spectroscopy. The use of both techniques gives new information about the structure and crystalline phases in the pure glassy and glass–ceramics systems. The iron atoms are present as Fe^{3+} and Fe^{2+} ions, and in both cases there is evidence that they are surrounded by six oxygen atoms (network modifier). The results suggest that the Nb ions occupy sites of average octahedral symmetry. Precipitation of ferroelectric crystalline phase of $LiNbO_3$ were detected.

There has been an increasing academic and technologic interest in glasses containing ferroelectric crystals as nonlinear optical materials [11,12]. Potassium niobate ($KNbO_3$) is among those oxide materials that respond to light-induced space charges by large changes in the refractive index. These crystals are well suited for photorefractive applications [11,12]. It is also a very interesting material for the study of the ferroelectric phase transitions, because it undergoes a cubic–tetragonal–orthorhombic–rhombohedral phase change sequence [13]. Moreover, contrary to other perovskite compounds such as $BaTiO_3$ and $PbTiO_3$, single domain samples can be available, in practice, in the four

* Corresponding author. Fax: +55-8-5287-4138.
E-mail address: sombra@ufc.br (A.S.B. Sombra).

0022-3697/00/$ - see front matter
PII: S0022-3697(99)00387-X

Table 1
Glass composition of the potassium niobophosphate system in mol%

Sample	K_2O	P_2O_5	Nb_2O_5	Fe_2O_3
A	50	50		
B	50	50		5
C	50	40	10	5
D	50	30	20	5
E	50	20	30	5
F	50	10	40	5
G	50		50	5

phases. The room temperature orthorhombic phase was specially investigated by neutron scattering [14], Raman scattering [15], and IR reflectivity experiments. For this and other reasons $KNbO_3$ has been extensively used for optical applications.

In this paper, we describe the fabrication of a series of potassium niobophosphate-based glasses, $[xNb_2O_5\cdot(50-x)P_2O_5\cdot 50K_2O]:yFe_2O_3$, with $0 \le x \le 50$ mol% and $y = 5$ mol%, and their characterization by X-ray diffraction, IR, Mössbauer, and Raman scattering spectroscopies. The main goal of the present work is to understand the formation processes of niobophosphate glass and glass ceramics and the role played by Fe_2O_3 in the structure of this material. Ferroelectric $KNbO_3$ was identified by the X-ray powder diffraction, Raman and IR spectra which are in agreement with previous data from the literature [13–15]. The potassium-niobate crystal $K_4Nb_6O_{17}$ were also identified by the X-ray diffraction, IR and Raman spectra for $x = 40$ and $x = 50$ mol%. The crystalline phase of KPO_3 was detected in sample A ($x = 0, y = 0$ mol%). Such glasses and glass-ceramics containing microcrystallites of ferroelectric materials formed in a controlled crystallization process would be interesting candidates for new optical nonlinear glasses or glass ceramics.

2. Experimental procedure

2.1. Glass preparation

Samples were prepared from reagent grade ammonium phosphate ($NH_4H_2PO_4$), potassium carbonate (K_2CO_3), niobium oxide (Nb_2O_5) and with iron oxide Fe_2O_3, by mixing reagents in appropriate proportions and heating them in platinum crucibles in an open electric furnace. The iron oxide Fe_2O_3 was included as an impurity. To prevent excessive boiling and consequent loss of mass, the water and ammonia in $NH_4H_2PO_4$ were removed by preheating the mixture at 200°C for several hours before the fusion. The mixture was subsequently melted at 1150°C for 1 h. The melt was then poured into a stainless steel mold and pressed between two stainless steel plates that yielded samples around 3 mm thick. The stainless steel plates did not receive any special polishing procedure. Batches to give ~10 g of each sample were prepared from the starting materials. The mold and plates were pre-heated to 300°C. The final glass compositions are $[xNb_2O_5\cdot(50-x)P_2O_5\cdot 50K_2O]:yFe_2O_3$, with $0 \le x \le 50$ mol% and $y = 5$ mol%. For details see Table 1.

Losses of K_2O and P_2O_5, which are the more volatile, due to our experimental procedure, were around 1.0 and 0.5 mol%, respectively, as measured by chemical gravimetric methods. A comparable loss has also been reported for lithium phosphate glasses [16], where loss of Li_2O is around 1–5 mol%. Because of the low loss detected in our sample preparation, the results are discussed in terms of the nominal starting compositions of the samples (Table1).

2.2. XRD

The X-ray diffraction (XRD) patterns were obtained at room temperature (300 K) by step scanning using powdered samples. We used five seconds for each step of counting time, with a Cu-Kα tube at 40 kV and 25 mA using the geometry of Bragg–Brentano.

2.3. Infrared spectroscopy

The IR spectra were measured using KBr pellets made from a mixture of powder for each glass composition. The pellet thickness varied from 0.5 to 0.6 mm. The IR spectra were measured from 400 to 1400 cm^{-1} with a Nicolet 5ZPX FT-IR spectrometer.

2.4. Mössbauer spectroscopy

The Mössbauer spectra were obtained in a standard transmission geometry, using a constant acceleration spectrometer with a radioactive source of ^{57}Co in Rh matrix. Measurements were carried out at room temperature on powder samples with absorber thickness 1.9 mg of natural iron per cm^2. The spectra were evaluated using the Normos fitting routine which makes use of a set of Lorentzian quadrupole doublets with fixed linewidth and isomer shift and computes the contribution of each curve to the total absorption spectrum by least square procedure. All the isomer shifts (δ) quoted are relative to metallic iron (α-Fe).

2.5. Raman spectroscopy

Raman spectra were measured with a laser Raman spectrometer using 5145 Å exciting light of the argon laser. The Raman scattering was measured in a back scattering geometry directly from the powder.

3. Results and discussion

3.1. IR and raman spectra

According to the X-ray powder diffraction (XRD) pattern (Fig. 1), sample A ($50K_2O–50P_2O_5$) is a ceramic where the

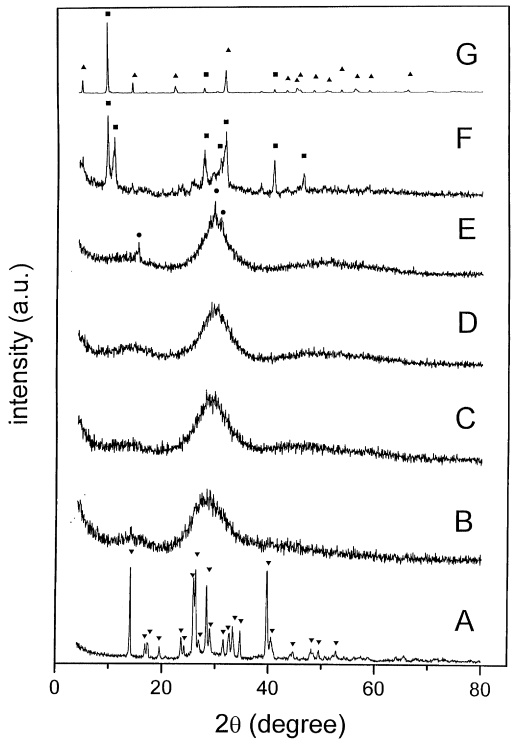

Fig. 1. The X-ray powder diffraction pattern of samples A–G (see Table 1): ▲—$KNbO_3$; ■—$K_4Nb_6O_{17}$; ●—unidentified phase; ▼—KPO_3.

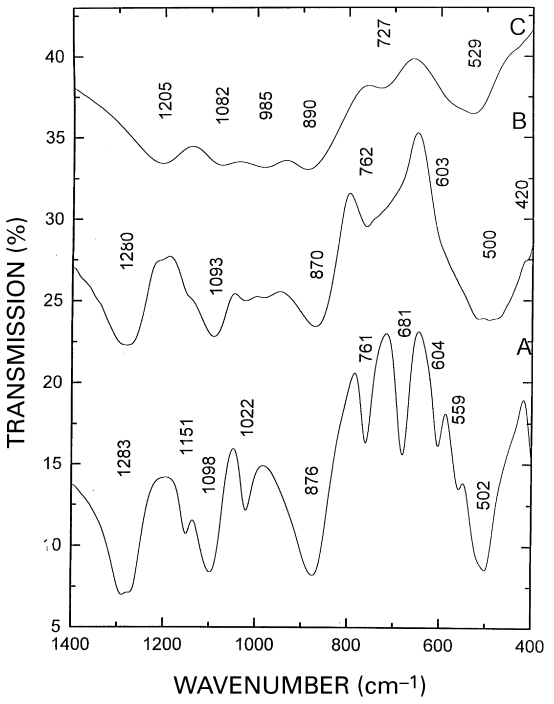

Fig. 2. Infrared spectra of the glasses A–C (see Table 1).

KPO_3 crystalline phase is easily identified. This is an expected result, according to the literature [17]. For the binary alkali-phosphate system, the maximum percentage allowed of the modifier (K_2O) is 47 mol% to obtain a glass sample. For our binary glass one has 50 mol% of K_2O resulting in the crystallization of the sample. However with the addition of 5 mol% of Fe_2O_3 we are again in the glass formation region. In Fig. 1 (Curve B) one has the same sample A with the addition of 5% Fe_2O_3. This curve is very characteristic of an amorphous material. Sample B ($50K_2O$–$50P_2O_5$:$5Fe_2O_3$), a basic composition to the glass family being studied, exhibits an amorphous phase. This is a strong indication that the addition of Fe_2O_3 is inducing the vitrification of this material. We believe that the iron oxide is working as a network former in this situation.

Mössbauer spectroscopy studies carried out in lithium niobo-phosphate glasses [10] show that in Nb_2O_5 containing glasses, the iron ions essentially occupy octahedra sites working as a network modifier. This observation is in agreement with other Mössbauer results reported in the literature [9]. However in sample B we believe that the iron oxide could have a network former characteristic. All the aspects of the iron behavior in this material will be studied during the analysis of the Mössbauer results.

Samples with x ranging from 0 to 20 mol% (Fig. 1, samples B, C and D) only exhibit an amorphous phase, whereas samples with $x = 30$ mol% (Fig. 1, sample E) exhibit, besides the amorphous phase, an additional crystalline phase (glass ceramics) which was not identified up to this point on our study [18,19]. We believe on the presence of niobium-phosphate structure in this phase. The ceramic characteristic of the samples is increasing with the ratio Nb_2O_5/P_2O_5. In sample F ($x = 40$ mol%) the phase $K_4Nb_6O_{17}$ was identified. In sample G ($x = 50$ mol%) the potassium niobate, $KNbO_3$ and $K_4Nb_6O_{17}$ are present.

Fig. 2 shows the IR spectra of samples A, B, and C. The absorption spectra of sample A could be directly associated with the spectra of the potassium metaphosphate (KPO_3) which is available in the literature [20]. A noticeable change is observed with the addition of 5 mol% of Fe_2O_3 for sample B. The IR spectra of sample B is characteristic of a phosphate glass. Assignment of the IR spectral features to phosphate-based glasses has been reported previously [21–23].

According to Muller [22], the absorption of the P=O group is around 1282–1205 cm^{-1} in polymeric phosphate chains. The stretching bands of $P–O^-$ (NBO, non-bridging oxygen) are around 1150/1050 and 950/925 cm^{-1}. Absorptions at 800/720 cm^{-1} are due to P–O–P vibrations (BO, bridging oxygen). The bands below 600 cm^{-1} are due to the bending mode of the PO_4 units in phosphate glasses.

Fig. 2 (Curve B) presents the IR spectrum of the basic potassium phosphate glass. Bands at 1280 cm^{-1} (P=O), 1093 and 870 cm^{-1} ($P–O^-$) and 762 and 500 cm^{-1} (P–O–P) are observed. However, the substitution of P_2O_5 by Nb_2O_5 (spectra C in Fig. 2) induces changes in the IR spectra. In

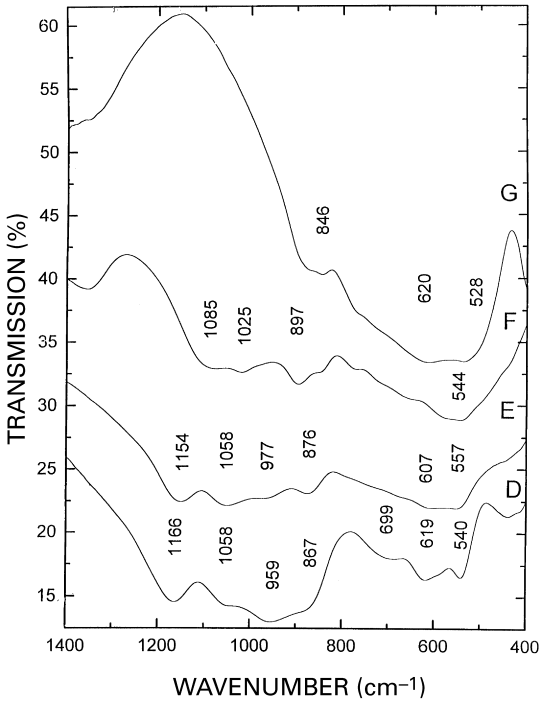

Fig. 3. Infrared spectra of the glass ceramics D–G (see Table 1).

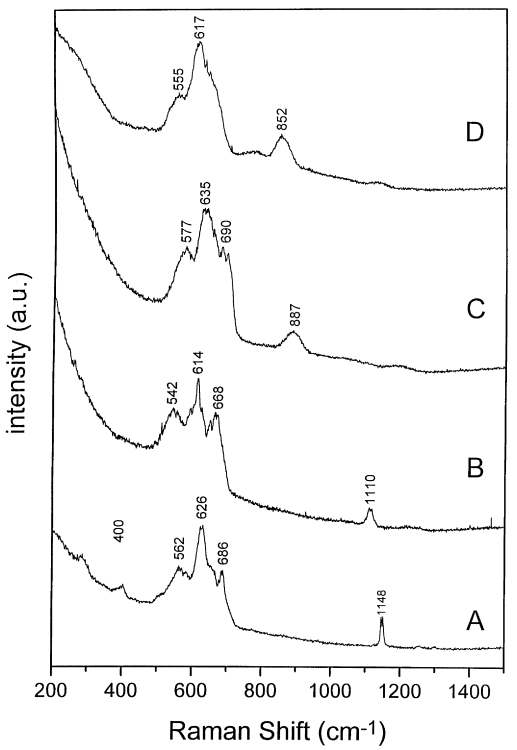

Fig. 4. Raman spectra of the samples A–D (see Table 1).

Fig. 3 (Curve D) the resonances associated with the bridging oxygen (P–O–P) around 727 and 529 cm^{-1}, for sample C, disappear and a new resonance appears around 600 cm^{-1} (spectrum D and E, Fig. 3). The absence of an IR absorption band near 1205 cm^{-1} in the samples D and E indicates the absence of the double bonded P=O. The resonances associated with the non-bridging oxygen ($P–O^-$) also decrease with the presence of the Nb_2O_5. This suggests that the niobium oxygen octahedra are using the NBO associated with phosphorus to form the glass network structure.

This observation is also supported by IR data [24], where NbO_6 octahedra exhibit absorption bands around 700 and 610/620 cm^{-1}. In our samples a broad band around 600 cm^{-1} is clearly observed in spectrum F and G of Fig. 3.

Fig. 3 shows the red spectra of the samples E, F, and G, corresponding to glass-ceramics and ceramics whose common characteristic is the presence of crystalline phases. Note that the IR spectra are strongly modified by this property. In spectra F, where we have the presence of P_2O_5 and Nb_2O_5, there are three major absorption bands around 1085, 1025 and 897 cm^{-1}, which are probably associated to differently arranged phosphorus-oxygen complexes in the material, and a broad band around 544 cm^{-1}. These former bands disappear in spectra G where the phosphorus is not present anymore. The broad band in the region of 528–620 cm^{-1} is probably associated with the formation of NbO_6 octahedra. The absorption bands around 1085 and 1025 cm^{-1}, for sample F, are associated with the ν_3 antisymmetric stretching vibration of the PO_4 tetrahedra. Reported studies in Li_3PO_4 crystal show that ν_3 are associated with two absorption bands of unequal intensity around 1093 and 1038 cm^{-1} and ν_4 is related to the absorption band around 600 cm^{-1} [25]. This doubling of ν_3 may result from some deformation of the PO_4 tetrahedra, or from vibrational coupling between anions in the same unit cell, or both. The detection of these absorption bands in the IR spectra of our glass ceramic samples indicates the presence of crystalline phases composed of structures with [PO_4] units. Note that in the spectrum G, of Fig. 3, where we do not have P_2O_5, the absorptions associated with the PO_4 tetrahedra are not observed. The absorption bands around 528 and 620 cm^{-1} in spectrum G are in good agreement with reported IR spectra of niobate glass ceramics [24]. These reported results show that the NbO_6 octahedra exhibit two major absorption bands at 700 and 610/620 cm^{-1}. These bands have been assigned to the ν_3 mode in the corner-shared NbO_6 octahedron [24,25]. All these assignments are supported by X-ray diffraction results. Fig. 1 shows the X-ray powder diffraction of the samples E, F and G. The crystallization of the niobate-phase $K_4Nb_6O_{17}$ is quite clear in sample F and decreases with increasing crystallization of $KNbO_3$, as shown in Fig. 3 (Curve G). If the niobium concentration is increased to $x = 50$ mol%, the $KNbO_3$ crystalline phase increases. In Fig. 1 (Curve G), the potassium niobate phase is easily identified.

To complete the vibrational mode information obtained

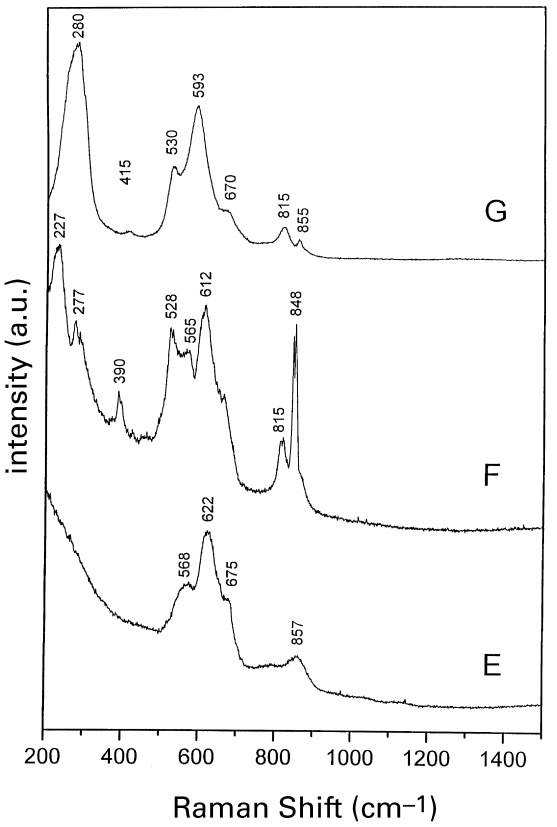

Fig. 5. Raman spectra of glass ceramics E–G (see Table 1).

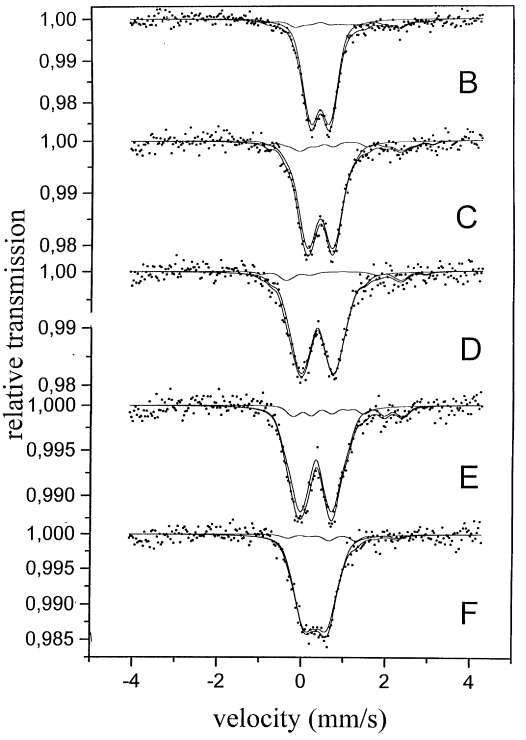

Fig. 6. Mössbauer spectra of the samples B–F (see Table 1) (●). Experimental points and the continuous line is the theoretical fitting.

with IR spectroscopy, we carried out room temperature Raman scattering measurements. These results are represented in Figs. 4 and 5, respectively. In spectrum A of Fig. 4 one has the typical Raman spectra of the KPO_3 crystalline phase. The two main peaks, 1148 and 686 cm^{-1} may be attributed to PO_4 groups. The chain type KPO_3 crystal exhibits the peak at 1148 cm^{-1}, which is assigned to the $\nu_s(PO_2)$-mode [26]. The peaks observed at 686, 626 and 562 cm^{-1} have been assigned to the symmetric P–O–P stretching vibration [ν(P–O–P)sym] of the symmetric PO_2 units. While the mode at 400 cm^{-1} are assigned to the O–P–O bending vibrational mode [ν(O–P–O)].

The 5 mol% of Fe_2O_3 impurity concentration, are present in all samples with exception of sample A. Sample B present modifications in the Raman spectra, comparing with sample A. The bands present some broadening effect which is characteristic of the glass structure.

The spectrum B of Fig. 4 show two major bands centered at 542, 614, 668 (ν_s(POP)-mode) and 1110 cm^{-1}($\nu_s(PO_2)$-mode). The spectrum C of Fig. 4, measured in the sample with 10 mol% of Nb_2O_5, shows three distinct peaks at 577, 635, 690 and 887 cm^{-1}. The 887 cm^{-1} peak has been previously assigned to a vibrational mode of Nb–O in octahedral NbO_6 or Nb–O–P [27]. Raman scattering studies of gallate glasses show peaks in the Raman shift range between 800 and 900 cm^{-1}, and between 600 and 800 cm^{-1}. The former Raman shift range has been attributed to highly distorted NbO_6 octahedra with non-bridging oxygen and the latter to a less-distorted NbO_6 octahedra with no non-bridging oxygen [8,28]. The 1110 cm^{-1} peak which was present in sample B (which is assigned to the $\nu_s(PO_2)$-mode) was not detectable in sample C anymore.

In Fig. 4 (Curve D) one has bands around 555, 617, and 852 cm^{-1}. The bands at 555 and 617 cm^{-1} ($\nu_s(PO_2)$-mode) could be associated to the phosphate structure, however we could expect some contribution from the niobium structure in this region of energy. The mode at 852 cm^{-1} is associated to the distorted NbO_6 octahedron with non-bridging oxygen. In Fig. 5 (Curve E) where we increase the ratio Nb_2O_5/P_2O_5 one can observe that the Raman spectra is quite similar to sample D. In samples E one has a glass ceramics, where the crystalline phase was not yet identified (see Fig. 1). In Fig. 5 (Curve F) one has the Raman spectra of the ceramics $K_4Nb_6O_{17}$. The spectrum F show a superposition of the modes from crystalline $K_4Nb_6O_{17}$ with vibrational modes from PO_4. The band that goes from 227 to 277 cm^{-1} is associated with PO_4 groups present in large part of the ceramic (vibration modes involving bending and torsional vibrations). The band around 528–612 cm^{-1} in potassium niobophosphate glasses, can be attributed to NbO_6 octahedral like in silicate glasses [28]. The broad band with

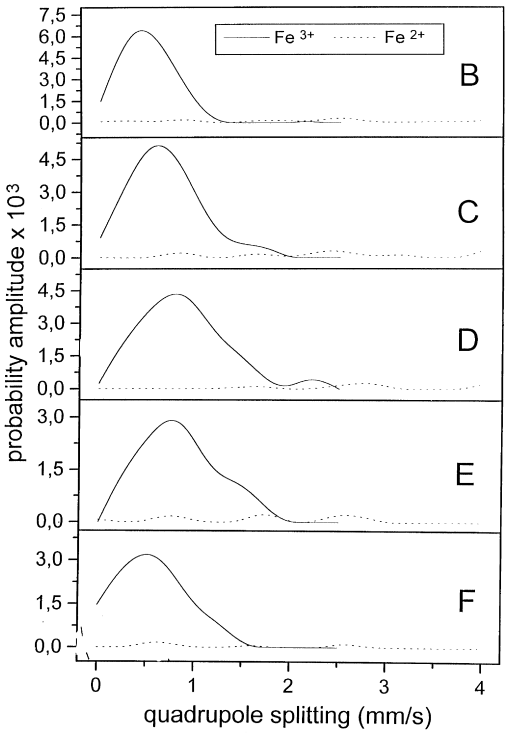

Fig. 7. Quadrupole splitting distribution for Fe^{3+} and Fe^{2+}.

peaks at 815 and 848 cm^{-1} is attributed to the NbO_6 octahedral with non-bridging oxygens with strong distortion.

In Fig. 5 (Curve G) one has the Raman spectra of the $KNbO_3$ ceramics. The peaks present are all associated to $KNbO_3$ in crystalline form [15]. The first band, which is centered at 280 cm^{-1}, is probably associated to the $A_1(\nu_{LO})$ mode which in the monocrystal is at 296 cm^{-1}. The peak at 415 cm^{-1} is also associated to the same phonon configuration $A_1(\nu_{LO})$ which in the crystal is at 417 cm^{-1} [15]. The other modes of the A_1(LO) phonons are present on the peaks at 530 and 815 cm^{-1}. The A_1(TO) phonons are present in the peaks at 593 cm^{-1}. The peak observed at 855 cm^{-1} is probably associated to the $K_4Nb_6O_{17}$ which is still present in sample G according with the X-ray diffraction (see Fig. 1).

3.2. Mössbauer spectra

In Figs. 6–8 show the Mössbauer spectra and the respective quadrupole splitting distributions, respectively, for samples B–G. All the spectra can be interpreted as the superposition of two broad doublets. The more intense doublet can be assigned, based on isomer shift and quadrupole splitting values, to high spin ferric iron (Fe^{3+}), and the less intense to high spin ferrous iron (Fe^{2+}) [10]. The Mössbauer spectra for sample G show, besides the paramagnetic doublets, two magnetic sextets component assigned to a Fe^{3+} magnetic phase. It is worth mentioning that, for all samples, we also recorded the high velocity spectra (±10 mm/s) to check the possibility of magnetic phases precipitation. However only for sample G these magnetic phases were detected.

For the paramagnetic phases of the spectra we used a set of 60 Lorentzian doublets, 30 to fit the Fe^{3+} contribution to the spectrum and 30 for the contribution of Fe^{2+}. The Lorentzian half width has been fixed to 0.12 mm/s, which is typical of a spectrum of standard metallic iron. In Table 2 are listed the Mössbauer parameters, isomer shift (δ), the most probable values of quadrupole splitting distributions (Δ_{max}) and the relative area population. According to Dyar [29] Fe^{3+} ions in an octahedral coordination [Fe^{3+}(VI)], present the Mössbauer parameter δ with values ranging from 0.35 to 0.55 mm/s relative to metallic iron, whereas for a tetrahedral coordination [Fe^{3+}(IV)] the δ value ranges from 0.20 to 0.30 mm/s. For Fe^{2+} ions, values of δ below 1.0 mm/s relative to metallic iron, are associated to tetrahedral coordination [Fe^{2+}(IV)] and values of δ above 1.0 mm/s are associated to octahedral coordination [Fe^{2+}(VI)]. The Mössbauer parameter quadrupole splitting (Δ) is also useful for evaluating the coordination number since a distorted tetrahedral site is characteristically less symmetric than a distorted octahedral site, therefore different values of Δ should be obtained. However it is observed

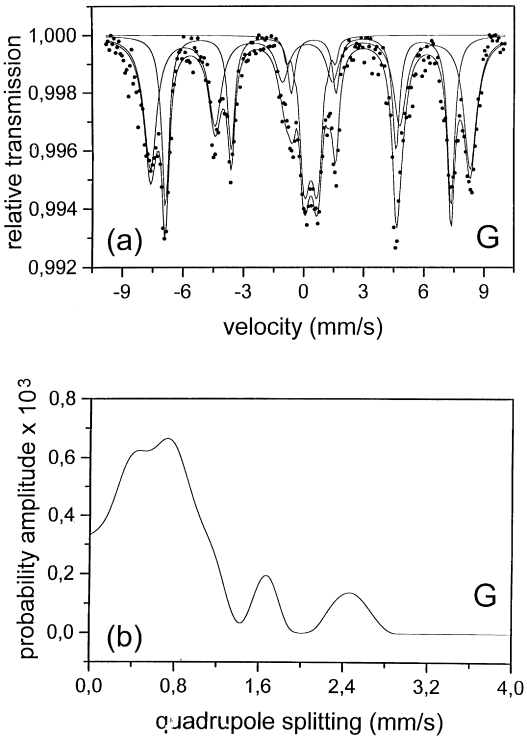

Fig. 8. (a) Mössbauer spectra of the sample G (see Table 1) (●). Experimental points and the continuous line is the theoretical fitting. (b) Quadrupole splitting distribution for Fe^{3+} and Fe^{2+}.

Table 2
Mössbauer parameters as obtained by the Normos [17] fitting program. This table shows the more probable values of quadrupole splitting (Δ_{max},), isomer shift (δ) and the absorption relative area %. δ is measured relative to metallic iron. The estimated error for all the Mössbauer parameters is around ± 0.01 mm/s

Sample	Site	Δ_{max} (mm/s)	δ (mm/s)	Area (%)
B	Fe^{2+}	–	1.05	17.3
	Fe^{3+}	0.44	0.39	82.7
C	Fe^{2+}	–	1.11	14.9
	Fe^{3+}	0.61	0.4	85.1
D	Fe^{2+}	–	0.95	9.1
	Fe^{3+}	0.81	0.34	90.9
E	Fe^{2+}	–	1.07	14.8
	Fe^{3+}	0.78	0.33	85.2
F	Fe^{2+}	–	0.96	8
	Fe^{3+}	0.54	0.34	92
G	Fe^{2+}	–	–	–
	Fe^{3+}	0.74	0.34	100
Fe^{3+} in a magnetic phase	Bhf = 49.4 T	0.15	0.25	
	Bhf = 44.2 T	0.26	0.35	

[29] that coordination number should be primarily determined from δ values. From Table 2 one can conclude that Fe^{3+} is the dominant ion with relative population bigger than 85% in average. In our case (see Table 2), for Fe^{3+} ions, the values of δ range from 0.33 to 0.40 mm/s and for Fe^{2+} ions δ varies from 0.95 to 1.11 mm/s. Therefore we can assume that both iron ions are at sites of distorted octahedral coordination, i. e. they could act as network modifiers (NWM). However the values obtained for δ are so close to the tetragonal coordination limit that we can not forget the possibility that the iron could be in a network former site. According to the X-ray results (Fig. 1) the presence of iron (5%) was enough to obtain vitrification of the material (sample B). The quadrupole splitting values are also in agreement with this interpretation.

Figs. 7 and 8 also shows the probability distributions of the Lorentzian doublets versus quadrupole splitting for Fe^{3+} and Fe^{2+} ions in samples B–G, respectively. As we can see, the distributions for Fe^{3+} are more intense compared to Fe^{2+} because of the relative amount of each ion. From this figure is quite clear that the quadrupole distribution of Fe^{3+} is very broad characteristic of an amorphous material. The distribution show one relative maxima of quadrupole splitting distribution (Δ_{max}), which are associated to different distortions of the octahedral symmetry around the iron ions. The position of the Δ_{max} represents the most probable value of the quadrupole splitting of the site. For sample B one has the presence of Fe^{3+} and Fe^{2+} ions. The Fe^{3+} ions which are 82.7% of the total iron, are in average site with $\Delta_{max} = 0.44$ mm/s. The Fe^{2+} ions in this sample (17.3% of the total iron) exhibit a low intensity doublet with a very broad distribution. With the increase of the Nb_2O_5, $x = 10$, 20 and 30%, there is a sizeable decrease of the Fe^{2+} population (from 17.3 to 9.1%). For sample D (20% Nb_2O_5) the maximum probability amplitude of Δ_{max} distribution for Fe^{3+} moved to a higher value (0.81 mm/s), meaning that the distortion of the Fe^{3+} sites increased. For samples E and F where the level of crystallinity increases (Fig. 1) the Δ_{max} value for the Fe^{3+} distribution decreases again, indicating that they are embedded in a more uniform structural and chemical neighborhood. These changes, for samples E and F, can certainly be ascribed to a formation of crystalline phases. In fact this was confirmed by X-ray diffraction results. The Mössbauer spectrum for sample G which shows, besides the paramagnetic doublets, two magnetic sextets component assigned to, based on isomer shift values, a magnetic phase associated to Fe^{3+} with hyperfine magnetic fields of 49.4 and 44.2 T. This magnetic phase was not identified up to this point in our study, however the existence of two hyperfine magnetic fields suggests that we might have an spinel structure for this phase [30].

4. Conclusions

Potassium niobophosphate glasses and glass-ceramics of the family $[xNb_2O_5\cdot(50-x)P_2O_5\cdot 50K_2O]{:}yFe_2O_3$ were studied by X-ray powder diffraction, IR, Mössbauer and Raman scattering spectroscopy. For the potassium-phosphate samples $[50P_2O_5{-}50K_2O]$ the iron oxide presents a network

former behavior, for 5 mol% of Fe_2O_3 doping. From our Mössbauer results, high spin Fe^{2+} and Fe^{3+} in a distorted octahedral coordination are present in all samples. One can conclude from the Mössbauer analysis that iron is present in a very broad site distribution, which is characteristic of an amorphous structural neighborhood. The precipitation of crystalline $K_4Nb_6O_{17}$ and the ferroelectric $KNbO_3$ crystals was confirmed by X-ray powder diffraction in the samples with $x = 40$ and 50 mol%, respectively. The IR and Raman scattering spectroscopy results suggest that the increase of the ratio Nb_2O_5/P_2O_5 leads the niobium to sites of octahedral symmetry and consequently to the formation of ferroelectric $KNbO_3$, as seen by X-ray diffraction analysis.

Acknowledgements

This work was partly sponsored by FINEP, CNPq (Brazilian agencies). We gratefully acknowledge the Centro de Tecnologia da UNIFOR (Universidade de Fortaleza) and NUTEC (Nucleo de Tecnologia do Ceará) for the use of their laboratories for sample preparation.

References

[1] E.M. Vogel, J. Am. Ceram. Soc. 72 (1989) 719.
[2] E.M. Vogel, S.G. Kosinski, D.M. Krol, J.L. Jacket, S.R. Friberg, M. Oliver, J.D. Powers, J. Non-Cryst. Solids 107 (1989) 244.
[3] A.S.B. Sombra, Solid State Commun. 88 (1993) 305.
[4] A.S.B. Sombra, Opt. Quantum Electron. 22 (1990) 335.
[5] A.S.B. Sombra, Braz. J. Phys. 24 (1994) 480.
[6] B. Samuneva, Kvalchev St., V. Dimitrov, J. Non-Cryst. Solids 129 (1991) 54.
[7] G.E. Rachkovskaya, N.M. Bubkova, J. Non-Cryst. Solids 90 (1987) 617.
[8] K. Fukumi, S. Sakka, J. Mater. Sci. 23 (1988) 2819.
[9] C.J. de Oliveira, et al., J. Mater. Sci. 28 (1993) 4305.
[10] E.B. de Araújo, J.A.C. de Paiva, M.A.B. de Araújo, A.S.B. Sombra, Phys. Status Solidi (b) 197 (1996) 231.
[11] T. Komatsu, et al., J. Non-Cryst. Solids 135 (1991) 105.
[12] P. Gunter, J.P. Huignard (Eds.), Photorefractive Materials and their Applications Springer, Berlin, 1988.
[13] R. Hewat, J. Phys. C. 6 (1973) 2559.
[14] C. Currat, R. Comes, B. Dorner, E. Wiesendanger, J. Phys. C 7 (1974) 2521.
[15] D.G. Bozinis, J.P. Hurrell, Phys. Ver. B. 13 (1976) 3109.
[16] M.M. Abouelleil, F.J. Leonberger, J. Am. Ceram. Soc. 72 (1989) 1311.
[17] A.K. Varshneya, Fundamentals of Inorganic Glasses, Academic Press, New York, 1994, 118 pp.
[18] J.A. Magalhaes de Abreu, J.A.C. de Paiva, R.S. Figueiredo, M.A.B. de Araujo, A.S.B. Sombra, Phys. Status Solidi (a) 162 (1997) 515.
[19] E.F. de Almeida, J.A.C. de Paiva, M.A.B. de Araujo, E.B. de Araujo, J.A. Eiras, A.S.B. Sombra, J. Phys.: Condens. Matter 10 (1998) 7511.
[20] R.A. Nyquist, R.O. Kagel, Infrared Spectra of Inorganic Compounds, Academic Press, New York, 1971, p. 154.
[21] D.E. Corbridge, E.J. Lowe, J. Chem. Soc. Part I (1954) 493.
[22] K.P. Muller, Glastechn. Ber. 42 (1969) 83.
[23] A. Mogus Milankovic, D.E. Day, J. Non-Cryst. Solids 162 (1993) 275.
[24] M. Tatsumisago, A. Hamada, T. Minami, M. Tanaka, J. Non-Cryst. Solids 56 (1983) 423.
[25] P. Tarte, J. Inorg. Nucl. Chem. 29 (1967) 915.
[26] C. Nelson, D.R. Tallant, Phys. Chem. Glasses 25 (1984) 31.
[27] A. El Jazouli, R. Brochu, J.C. Viala, R. Olazcuaga, C. Delmas, G. Le Flem, Ann. Chim. Fr. 7 (1982) 285–292.
[28] K. Fukumi, T. Kokubo, K. Kamiya, S. Sakka, J. Non-Cryst. Solids 84 (1986) 100.
[29] M.D. Dyar, Am. Mineralogist 70 (1995) 304.
[30] H.A. Maia, F.F.T. de Araujo, M.A.B. de Araujo, J. Danon, R.B. Frenkel, Hyperfine Interactions 77 (1993) 43.